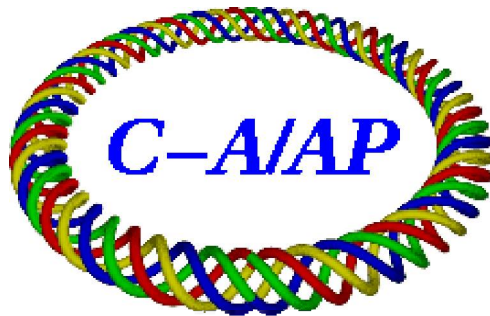# Exploring a possible origin of a 14 deg y-normal spin $\vec{n}_0$ tilt at RHIC polarimeter

F. Meot, H. Huang

Collider-Accelerator Department
Brookhaven National Laboratory
Upton, NY 11973

U.S. Department of Energy
Office of Science, Office of Nuclear Physics

Exploring a possible origin of a 14 deg y-normal spin $\vec{n}_0$ tilt at RHIC polarimeter.

F. Méot, H. Huang

BNL C-AD, Upton, LI, NY 11973

June 2015

Abstract

A possible origin of a 14 deg y-normal spin $\vec{n}_0$ tilt at the polarimeter is in snake angle defects. This possible cause is investigated by scanning the snake axis angle μ, and the spin rotation angle at the snake, ϕ, in the vicinity of their nominal values.

Tech Note C-A/AP/538

Contents

1   Introduction

In recent analysis of run13 p-carbon polarimeter measurements, it was found that spin angle was significantly tilted away from vertical. The measurements showed that this was the case at both injection and store of 255 GeV. A possible origin of a 14 deg y-normal spin $\vec{n}_0$ tilt at the polarimeter is in snake angle defects. This possible cause is investigated by scanning the snake axis angle μ, and the spin rotation angle at the snake, ϕ, in the vicinity of their nominal values.

2   Working hypotheses

- Blue ring is considered, The origin of the Zgoubi input data file is from translation of the MADX "blue holy lattice". It also happens to be the very file used for earlier spin tracking studies which can be referred to if necessary, in particular, "Effect of snake rotation angle error on spin transmission through 411-Qy", June 2011 spin meeting.

- 255 GeV store is considered, with two different optics, called "Run 13" or "pp11v7" in the following.

- The game in this study consists in changing (i) the orientation of the snake axes, which are contained in the plane of the ring with μ_1, μ_2 their angle to the beam axis, and (ii) the spin rotation angle at the snakes, ϕ_1, ϕ_2, within the following limits :

    - snake axes are maintained at constant $\Delta\mu = 90$ degrees from one another (the design value)
    - ϕ_1 and ϕ_2 are moved away from the 180 degrees design value independently from one another.

- For any (μ, ϕ) arrangement, just one set of random orbit defects is run : it remains to be confirmed that this does give a correct idea of the value of the y-normal tilt of spin $\vec{n}_0$ around the ring (by y-normal, it is meant a rotation with axis contained in the horizontal plane, which moves $\vec{n}_0$ away from the vertical).

Method :

A fitting procedure is used to find $\vec{n}_0$ from the lattice once the snake axis angles μ_1, μ_2 or the snake angles ϕ_1, ϕ_2 have been moved.

3   "Run 13 optics"

The optics of concern is summarized in Figs. 1-4. In these simulations a vertical orbit may be considered, in that case it is scaled from that displayed in Fig. 1; the horizontal orbit is scaled similarly, with the same *rms* value.

3.1   Case of zero vertical orbit

In these μ and ϕ scans, the orientation of snake 1 axis takes the values $\mu_1 : -90 \rightarrow +90$ deg. (step 45 deg.) whereas snake 2 axis takes the values $\mu_2 = \mu_1 - 90$ deg.
The spin rotation angle ϕ takes its values between 160 and 200 deg., for both snakes.
This generates the set of curves below.

"Run 13" optics,
including vertical orbit (corrected from 29th harmonic)

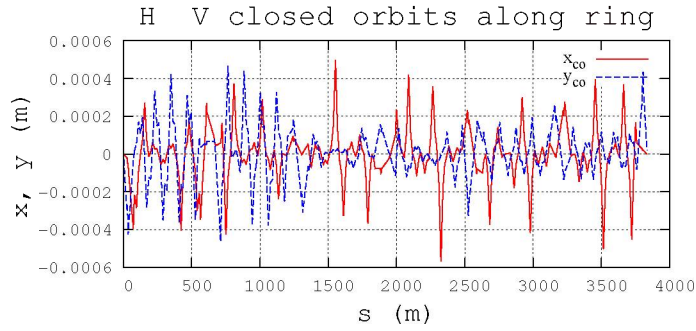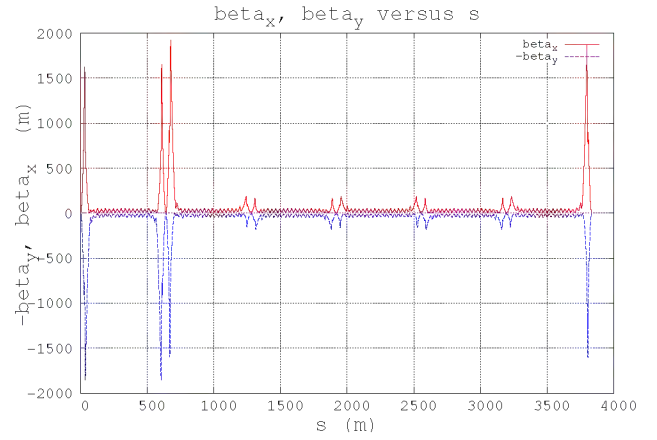Figure 1: H and V orbits. The *rms* value of the vertical orbit in the arcs is 25μm.

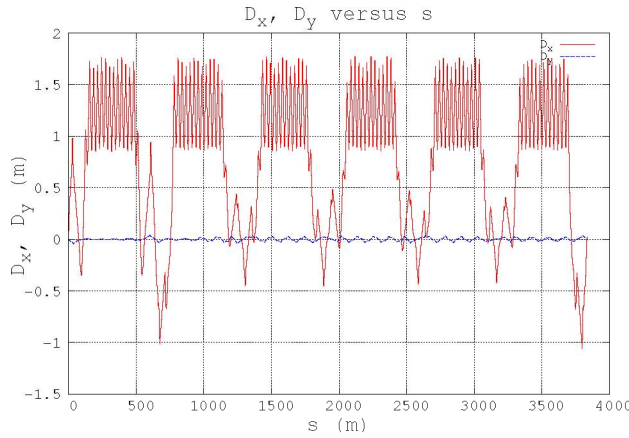Figure 2: Horizontal and vertical optical functions.
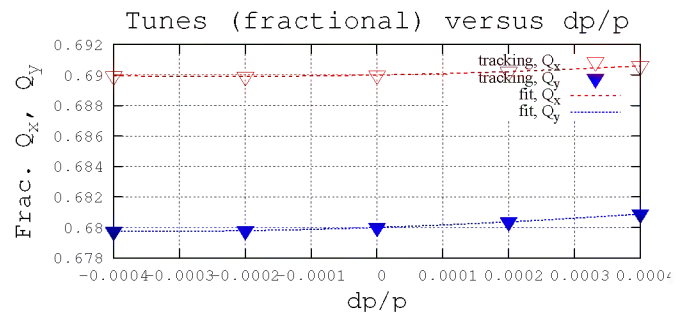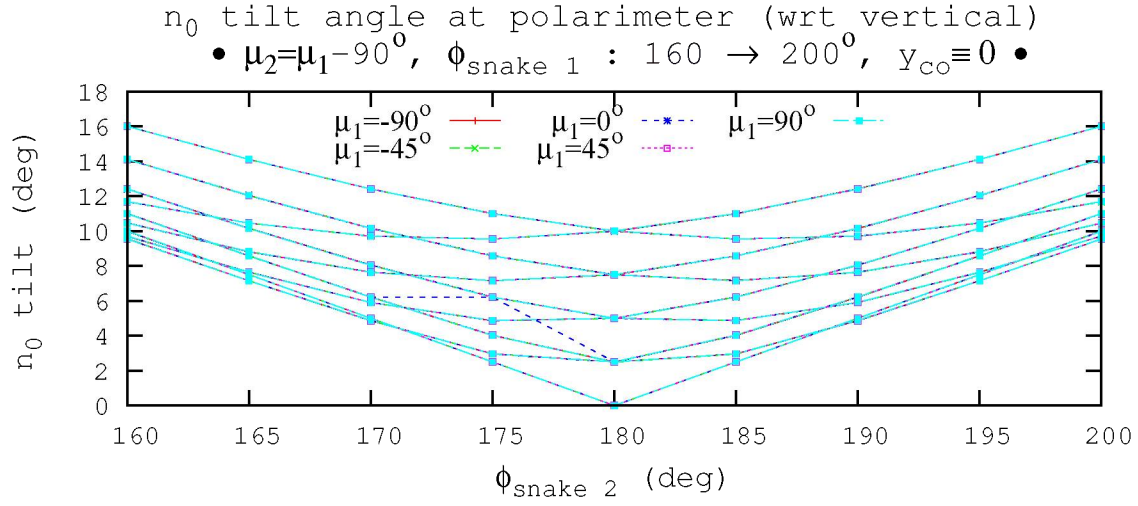

Figure 3: Horizontal and vertical dispersions.

Figure 4: Momentum dependence of tunes, and matching polynomials $Q(\delta) = Q_0 + Q'\delta + Q''\delta^2 + Q'''\delta^3$.
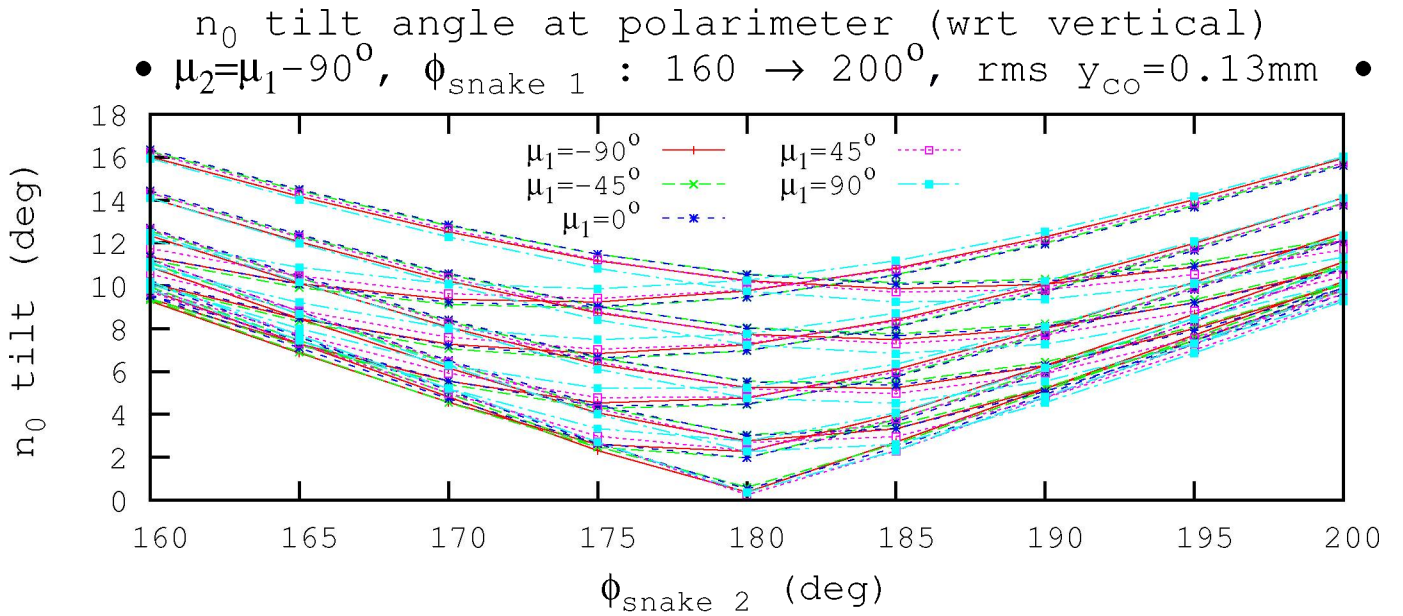
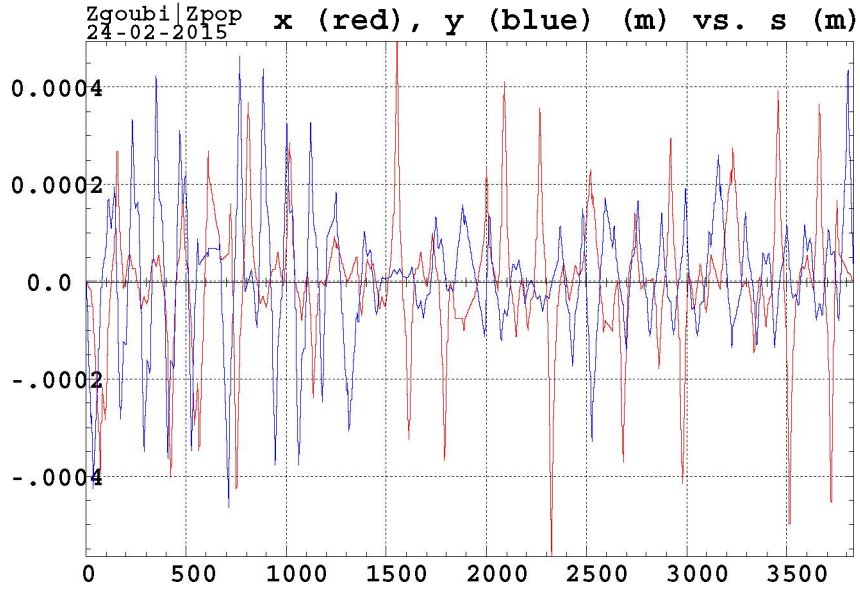n_0 tilt angle at polarimeter (wrt vertical)

$\bullet \ \mu_2 = \mu_1 - 90^o, \ \phi_{snake\ 1} : 160 \to 200^o, \ y_{co} \equiv 0 \ \bullet$

Details of some of the numerical values in the figure above :

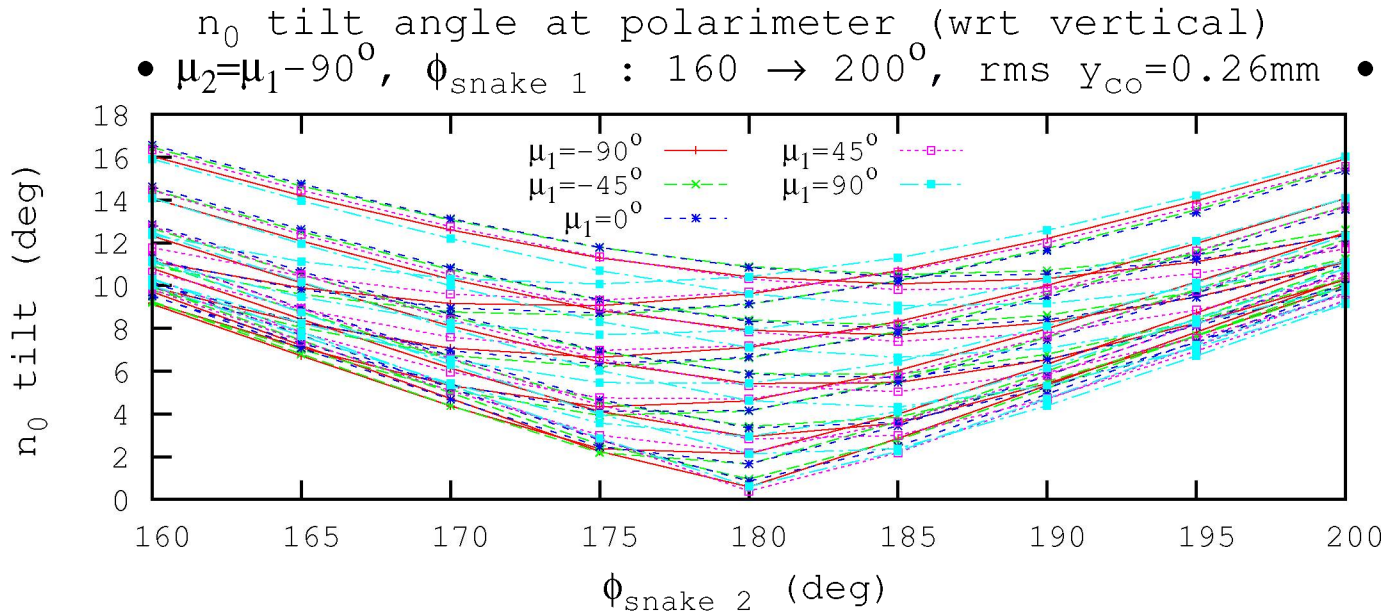| mu_2+90 =mu_1 deg.	phi_1 deg.	phi_2 deg.	------- @ clock6 ----------			------- angle to y axis ---------		
			n_0_l	n_0_x	n_0_y	@clock6 deg.	@PJET deg.	@Polarmtr deg.
45.	170.	170.	-0.0354	0.0965	0.9948	5.8372	171.9635	171.9635
45.	170.	180.	-0.0838	0.0244	0.9963	4.9328	175.0065	175.0065
45.	170.	190.	-0.1314	-0.0479	0.9901	8.0593	174.1027	174.1027
45.	180.	170.	0.0483	0.0726	0.9963	4.9328	174.9980	174.9980
45.	180.	180.	-0.0001	0.	1.	0.	180.	180.0000
45.	180.	190.	-0.0482	-0.0726	0.9963	4.9328	175.0006	175.0006
45.	190.	170.	0.1314	0.0481	0.9901	8.0593	174.0938	174.0938
45.	190.	180.	0.0837	-0.0244	0.9962	4.9873	175.0011	175.0011
45.	190.	190.	0.0353	-0.0965	0.9947	5.8834	171.9607	171.9607
45.	160.	160.	-0.0695	0.1904	0.9793	11.6897	163.9927	163.9927
45.	160.	165.	-0.0942	0.1553	0.9835	10.4363	165.8937	165.8937
45.	160.	170.	-0.1186	0.1198	0.9857	9.7083	167.5955	167.5955
45.	160.	175.	-0.1428	0.0844	0.9862	9.5390	169.0043	169.0043
45.	160.	180.	-0.1667	0.0486	0.9849	9.9568	170.0015	170.0015
45.	160.	185.	-0.1905	0.0128	0.9817	10.9696	170.4618	170.4618
45.	160.	190.	-0.2137	-0.0230	0.9765	12.4344	170.2988	170.2988
45.	160.	195.	-0.2366	-0.0588	0.9699	14.0989	169.5475	169.5475
45.	160.	200.	-0.2588	-0.0946	0.9612	16.0056	168.3069	168.3069

3.2   Case of a 0.13 mm *rms* vertical orbit

In these μ and ϕ scans, the vertical orbit is scaled from that displayed in Fig. 1, with an *rms* value of 0.13 mm. The *rms* horizontal orbit is 0.13 mm as well.
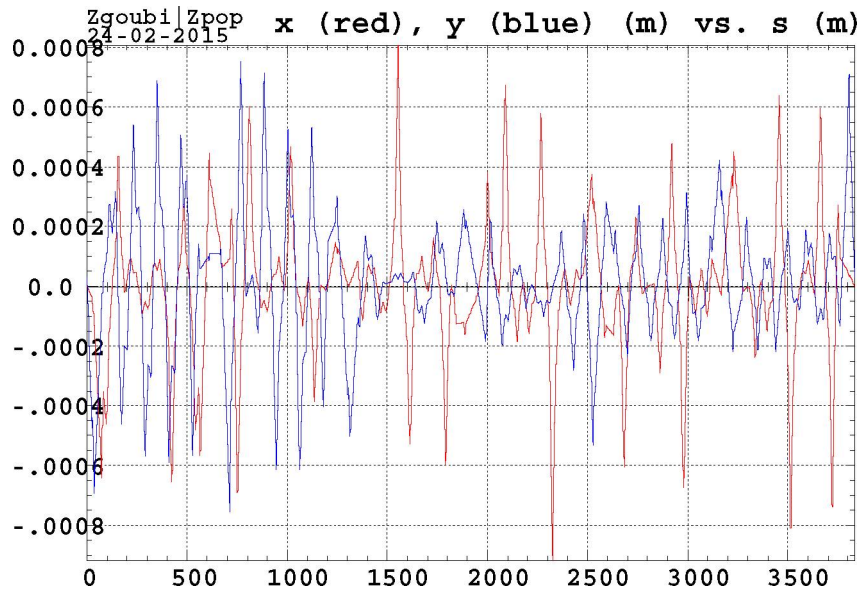
3.3   Case of a 0.26 mm *rms* vertical orbit

In these μ and ϕ scans, the vertical orbit is scaled from that displayed in Fig. 1, with an *rms* value of 0.26 mm. The *rms* horizontal orbit is 0.26 mm as well.

4   Case of "pp11v7 optics"

This optics is that of the ramp and includes vertical separation bumps at IPs. Although this is not the conditions for the polarization measurements addressed here, the interest is to assess a possible effect of such bumps.

Working conditions in this "pp11v7" style optics are displayed in Figs. 5-8. They are the same as in the spin tracking simulations presented at the Nov. 2011 spin meeting, which can be referred to for details.

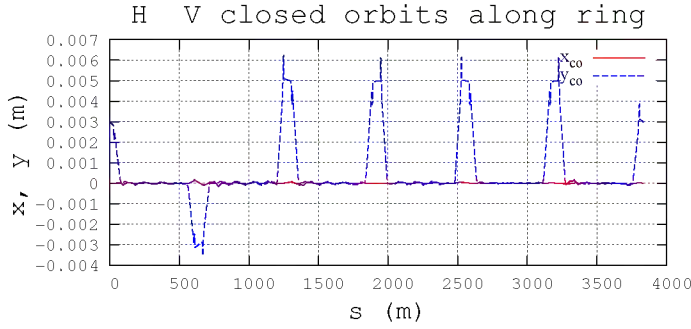**"pp11v7 optics",**
including vertical separation bumps at IPs

Figure 5: H and V orbits. The rms value of the vertical orbit in the arcs is 25μm.
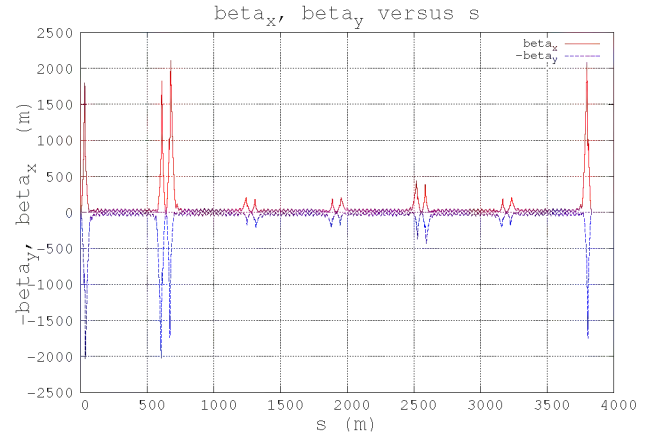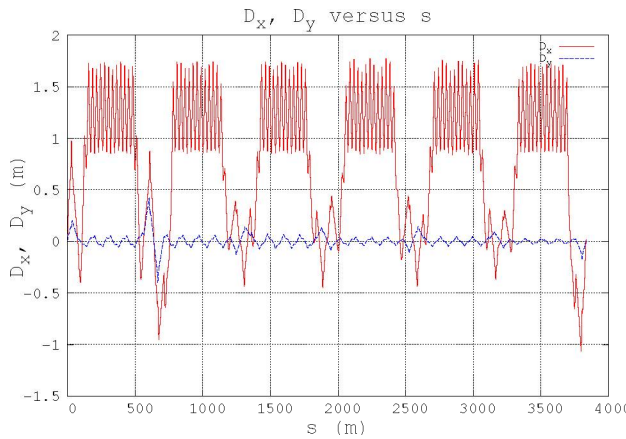
Figure 6: Horizontal and vertical optical functions.
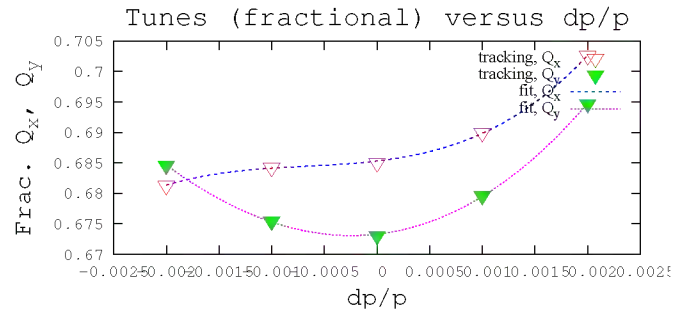
Figure 7: Horizontal and vertical dispersions.

Figure 8: Momentum dependence of tunes, and matching polynomials $Q(\delta) = Q_0 + Q'\delta + Q''\delta^2 + Q'''\delta^3$.
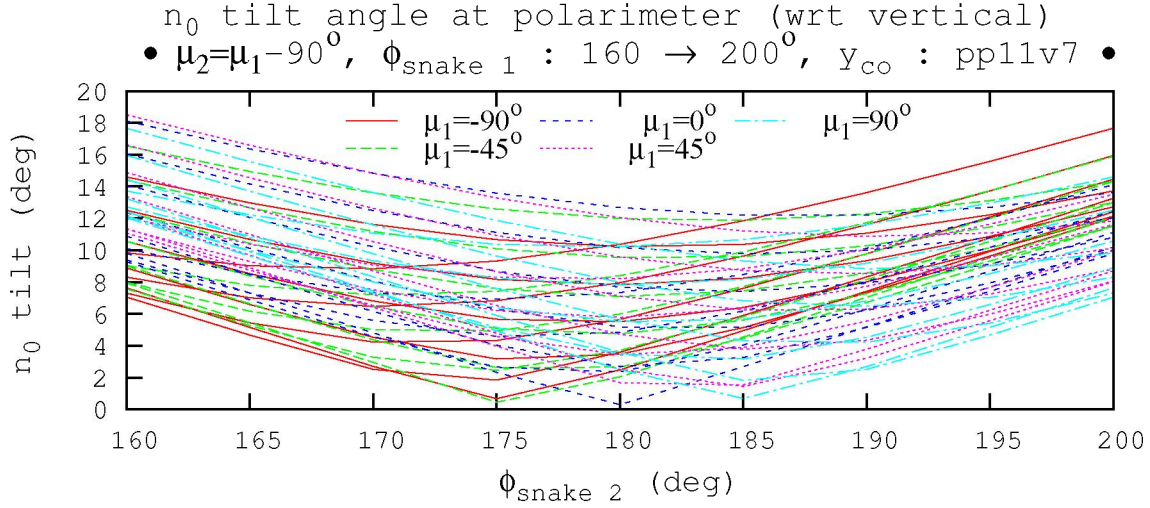
Horizontal : $Q_x = 0.6853$, $Q'_x = 2.037$
Vertical : $Q_y = 0.6732$, $Q'_y = 1.950$

4.1   Case of vertical separation bumps at all IPs

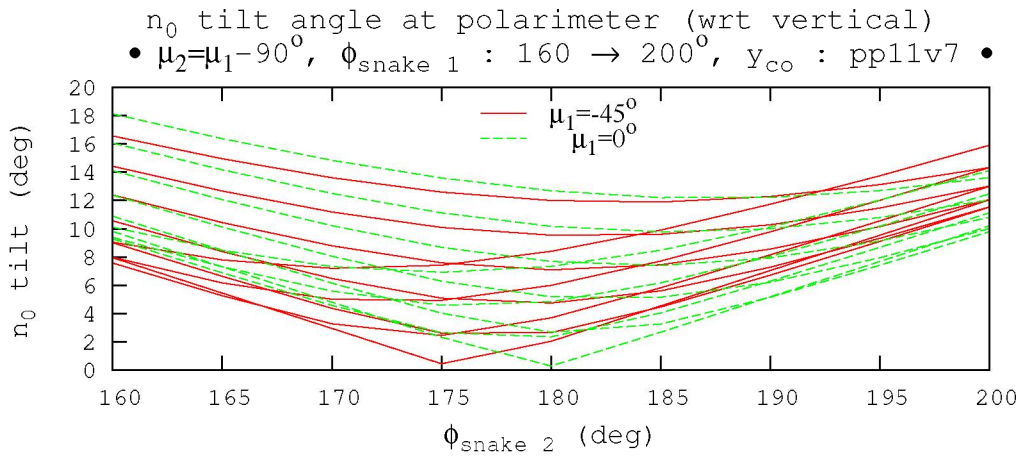In these μ and ϕ scans, the orientation of snake 1 axis takes the values $\mu_1 : -90 \rightarrow +90$ deg. (step 45 deg.) whereas snake 2 axis angle takes the values $\mu_2 = \mu_1 - 90$ deg.

The spin rotation angle ϕ takes its values between 160 and 200 deg., for both snakes.

This generates the set of curves below.

The graph below is an excerpt of the one above, for clarification.

The table below gives details regarding the curves displayed in the previous figures.

mu_2+90 =mu_1 deg.	phi_1 deg.	phi_2 deg.	n_0_l	n_0_x	n_0_y	@clock6 deg.	@PJET deg.	@Polarmtr deg.
45.	170.	170.	-0.0308	0.0914	0.9953	5.5521	172.2901	169.4557
45.	170.	180.	-0.0789	0.0191	0.9965	4.7653	175.1204	172.8754
45.	170.	190.	-0.1268	-0.0533	0.9904	7.9577	173.8732	173.7120
45	180.	170.	0.0528	0.0674	0.9963	4.9328	175.3964	172.7744
45.	180.	180.	0.0047	-0.0052	1.	0.	179.6053	177.4910
45.	180.	190.	-0.0437	-0.0778	0.9960	5.0945	174.6010	176.7851
45	190.	170.	0.1360	0.0427	0.9899	8.1596	174.3120	173.4801
45.	190.	180.	0.0884	-0.0296	0.9956	5.4039	174.8511	176.5602
45.	190.	190.	0.0400	-0.1020	0.9941	6.2406	171.6190	174.4574
0.	170.	170.	0.0452	0.0853	0.9953	5.5521	172.1957	169.7911
0.	170.	180.	-0.0401	0.0684	0.9969	4.5326	175.1808	172.3233
0.	170.	190.	-0.1250	0.0511	0.9909	7.7157	174.0857	172.0715
0.	180.	170.	0.0872	0.0092	0.9962	4.9873	175.2045	173.8502
0.	180.	180.	0.0018	-0.0081	1.	0.	179.7569	177.3158
0.	180.	190.	-0.0836	-0.0253	0.9960	5.0945	174.7913	174.8439
0.	190.	170.	0.1285	-0.0671	0.9894	8.3566	174.1230	175.4307
0.	190.	180.	0.0435	-0.0844	0.9956	5.4039	174.8045	177.6496
0.	190.	190.	-0.0416	-0.1014	0.9941	6.2406	171.7121	173.7038

Tilt angle between $\vec{n}_0$(PJET) and $\vec{n}_0$(Polarimeter)

PJET and polarimeter are at respectively 1917.39376 m, 1988.53985 m (see next two figures), 71 m distant from one another. In addition,
- PJET is on the y_{co}-plateau,
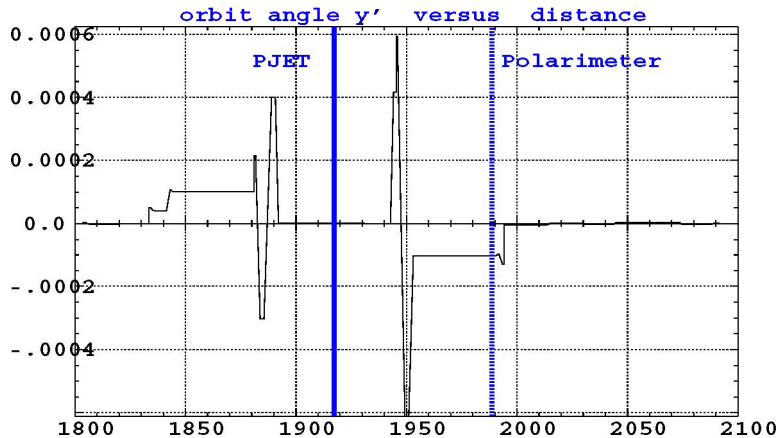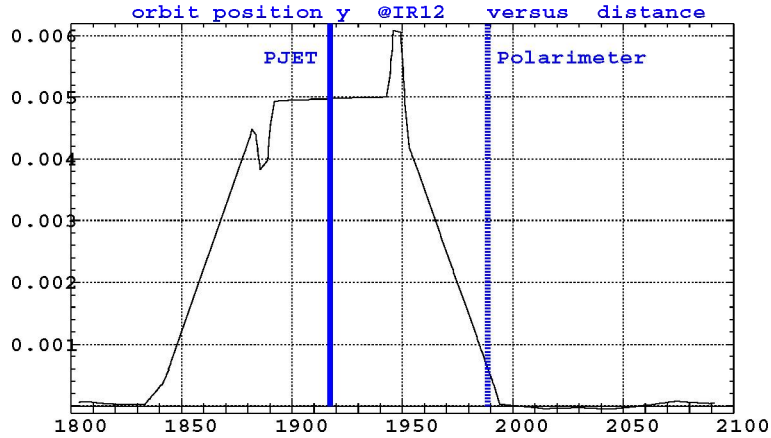- the polarimeter is at the downstream end of the y_{co} bump,

This is schemed in the two figures below : the first one shows the orbit amplitude, the second one shows the orbit angle, as a function of the distance along the ring.

Due to the vertical orbit, $\vec{n}_0$ undergoes a y-tilt which amounts to the integrated $G\gamma\alpha$.

From the tracking, the values of concern are as follows :
- the relative vertical orbit deviation between PJET and polarimeter is (ramp optics) $\alpha \approx 0.1$ mrad, $G\gamma\alpha \approx$ 49 mrad = 2.8 deg, not far from the 2.1 deg as of the tracking for $\mu_1 = -\mu_2 = 45$ deg, $\phi_1 = \phi_2 = 180$ deg, previous page.

Scaling down to actual beam separation during store of about half less, i.e., $\alpha \approx 0.1$ mrad $\rightarrow 0.05$ mrad, the result is half as much, namely a $\boxed{\sim 1.4 \text{ deg}}$ spin tilt difference between PJET and polarimeter.

4.2   Case of zeroed vertical bumps at IPs 6, 8

Compared to the previous section the vertical bumps at IPs 6, 8 are zeroed here, figure below, so corresponding to collision conditions.
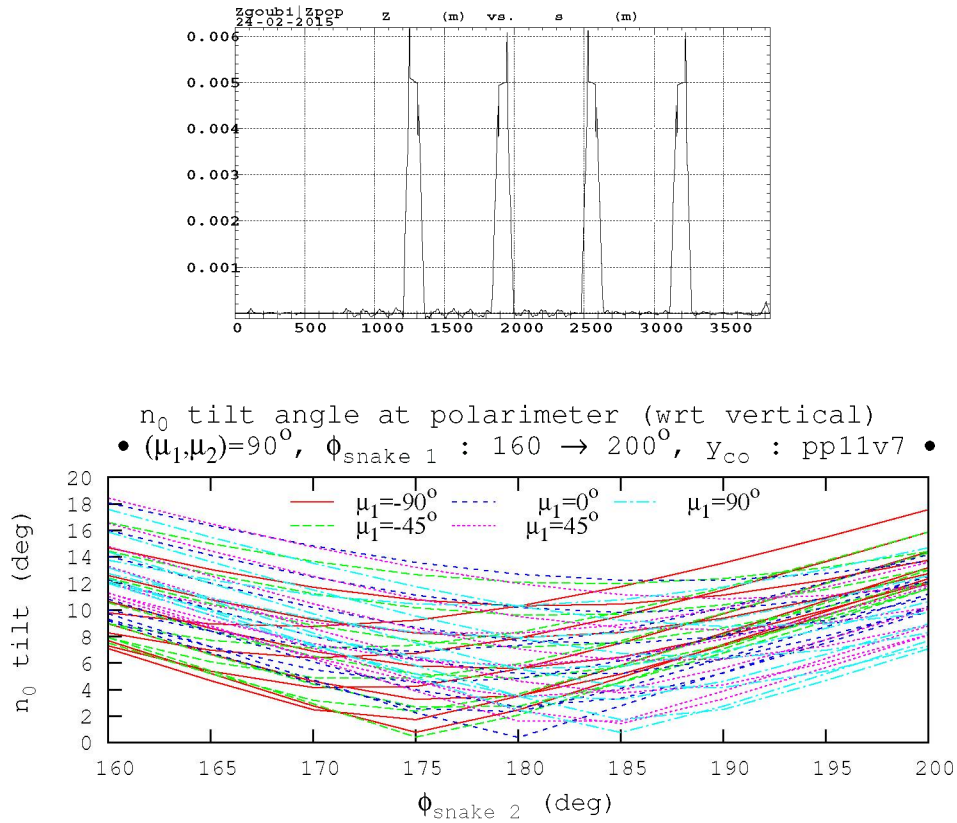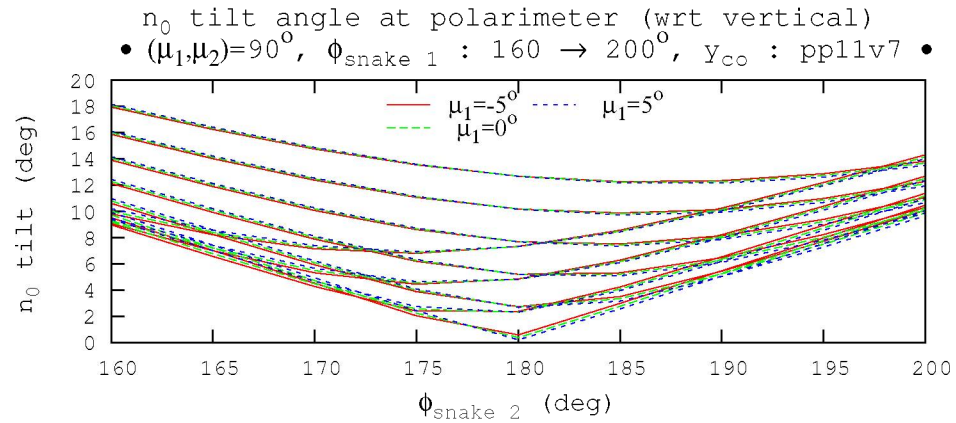

Figure below : previous case limited to $\mu_1 = 0, \ \pm 5$ deg.

5   Summary

Assuming correct orientation of the spin precession axes, +45 and -45 deg at snake 1, 2 respectively, the following is learned from these snake axis and spin angle scans :

- In the presence of the vertical separation bumps, a ± 10 deg. error on the snake angles ϕ_1, ϕ_2 may entail ~ 11 deg. $y^\perp$-tilt of spin $\vec{n}_0$ at the polarimeter (see page 10).

- In the absence of the separation bumps the effect is ~ 8 deg (see page 5).

- A defect of ± 5 deg in the orientation of the spin precession axis (see page 12) marginally impacts on what precedes.